

RESEARCH

Open Access



# Deformation of brain in normal pressure hydrocephalus is more readily associated with slow vasomotion rather than heartbeat related pulsations of intracranial pressure

Ronald T. Murambi<sup>1,2†</sup>, Henora Chour<sup>3</sup>, Magdalena Kasproicz<sup>4</sup>, Craig R. Vonhoff<sup>1,2</sup>, Marek Czosnyka<sup>5,6</sup>, Zofia Czosnyka<sup>5</sup> and Matthias Jaeger<sup>1,2\*†</sup>

## Abstract

**Objective** Enlarged brain ventricles, compressed parasagittal cerebrospinal fluid spaces, steep callosal angle, dilated sylvian fissures and focal cortical sulcal dilatation are typical imaging features of idiopathic normal pressure hydrocephalus (iNPH). The pathophysiological mechanisms behind these morphological changes are poorly understood, but the hydrodynamic concepts of communicating hydrocephalus suggest that increased heartbeat related intracranial pulsations are involved in ventricular enlargement. In this cross-sectional study we analysed the association between the radiological findings of iNPH and the physiological intracranial pressure (ICP) waveform components.

**Methods** 117 patients with suspected iNPH underwent computerised overnight ICP monitoring with calculation of heartbeat related ICP pulse wave amplitude (calculated in the frequency domain, AMP, and time domain, MWA), amplitude of respiration induced ICP waves (RESP), power of slow vasogenic waves (SLOW), and index of cerebrospinal compensatory reserve (RAP). Radiological morphological data was recorded from computed tomography using Evans Index (EI), frontal occipital horn ratio (FOHR), and disproportionately enlarged subarachnoid space hydrocephalus (DESH) score.

**Results** The strongest correlation was observed between SLOW and DESH ( $r=0.44$ ,  $p<0.012$ ). SLOW also correlated with ventricular size as measured with EI ( $r=0.23$ ,  $p=0.045$ ) and FOHR ( $r=0.26$ ,  $p=0.037$ ). ICP and RESP also correlated with DESH ( $r=0.25$ ,  $p=0.037$  and  $r=0.25$ ,  $p=0.038$ , respectively). AMP and MWA were not correlated with the radiological data.

**Conclusions** Mainly SLOW showed correlations with the morphological imaging features of iNPH. SLOW is influenced by vasomotion and intracranial compliance. This study suggests that the magnitude of ICP slow wave activity, but not ICP pulse component is related to the size of brain ventricles and DESH in iNPH.

**Keywords** Idiopathic normal pressure hydrocephalus, Intracranial pressure, Neuromonitoring, Intracranial compliance, Intracranial pulsations, Computed tomography

<sup>†</sup>Ronald T. Murambi and Matthias Jaeger contributed equally to this work.

\*Correspondence:

Matthias Jaeger

matthias.jaeger@health.nsw.gov.au

Full list of author information is available at the end of the article



## Introduction

Idiopathic normal pressure hydrocephalus (iNPH) is a neurodegenerative disease occurring in the aging population. It is characterised by a clinical triad of progressive gait impairment, decline in cognitive function and incontinence. The natural history of iNPH is unfavourable with worsening neurological symptoms and reduced survival [1, 2]. The treatment is surgical insertion of a ventriculo-peritoneal, ventriculo-atrial or lumbo-peritoneal shunt, which can lead to improved symptoms in selected patients [3, 4]. Delays in surgical treatment lead to disease progression and increased risk of unfavourable outcome [5].

The pathophysiological processes of iNPH are incompletely understood, but it is now well accepted that iNPH represents a complex disturbance of cerebrospinal fluid (CSF) dynamics with normal baseline intracranial pressure (ICP) that becomes symptomatic at the late stages of life. Initial findings that increased resistance to CSF outflow is the main mechanism standing behind the development of iNPH were later challenged [6, 7]. A lack of clear diagnostic criteria makes selection of patients for surgical treatment and differentiation from other neurodegenerative diseases difficult. Current evidence indicates that iNPH is mainly underdiagnosed and undertreated [8], but patients may also be subjected to CSF diversion surgery without sustained neurological improvement [9–11].

Enlarged brain ventricles on computed tomography (CT) or magnetic resonance imaging (MRI) without evidence of obstruction of CSF flow are the radiological hallmark of iNPH and one of the main diagnostic criteria in clinical practice. In addition, morphological features such as an acute callosal angle, compressed parasagittal CSF spaces, dilated sylvian fissures and focal cortical sulcal dilatation have been described as typical imaging findings in iNPH, often summarised as disproportionately enlarged subarachnoid space hydrocephalus (DESH) [12].

Despite the important role of these radiological findings to select patients with suspected iNPH for surgery, it is still unclear why the ventricles enlarge in iNPH in the absence of CSF flow obstruction and normal ICP. More so, it remains elusive why the DESH changes occur and what pathophysiological mechanisms are behind these morphological characteristics of iNPH.

The monitoring of ICP and its waveform components has long been used for the diagnostic management of iNPH [13–15]. ICP is derived from cerebral blood and CSF circulatory dynamics and can provide physiological information about cerebrospinal reserve capacity, compliance, and vasogenic components. Some ICP waveform changes have been associated with iNPH, such as increase of the heartbeat related pulse pressure amplitude

or vasogenic slow wave (also termed “b-wave”) activity [16–20]. In fact, elevations of the heartbeat related ICP pulse pressure amplitude have been thought to be involved in the development of ventricular enlargement in hydrocephalus, sometimes termed the “water-hammer” effect as part of the hydrodynamic pathophysiological model of communicating hydrocephalus [7, 21–23].

The aim of this study was to analyse the relationship between the characteristic morphological findings of iNPH on brain imaging (ventricular enlargement, DESH), and the physiological ICP signal with its waveform components from diagnostic overnight monitoring. While our study was largely exploratory, we hypothesised that, consistent with the hydrodynamic theories of hydrocephalus pathophysiology, an association between the ICP derived intracranial heartbeat related pulsations and ventricle size might exist.

## Methods

### Patient characteristics

We included patients undergoing diagnostic ICP monitoring as part of routine clinical investigation for iNPH under the care of the senior author from 2010 to 2021. Patients were identified from the hydrocephalus ICP monitoring database, the selection process is described in Fig. 1. Patients had probable or possible iNPH as described in the iNPH-guidelines [24], meaning they had ventricular enlargement on CT and MRI brain imaging without evidence of CSF flow obstruction, together with appropriate clinical findings and no history of other causes of secondary NPH, such as brain haemorrhage or infection. The disease severity was assessed by one of the authors (MJ) using the Oslo-iNPH grading scale [25]. This scale allocates 1–5 points according to disease severity to each of the three domains of iNPH, gait

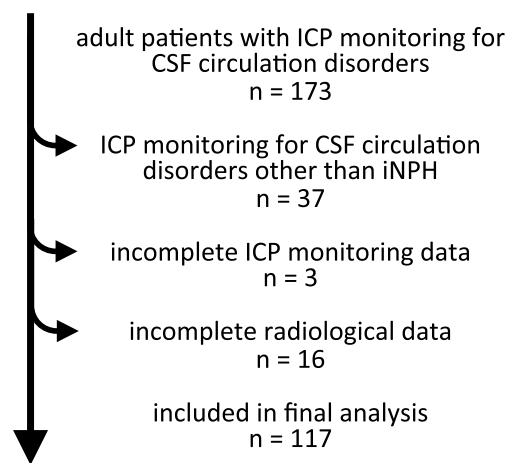


**Fig. 1** Selection process for the study population

impairment, cognitive impairment and incontinence. Patients receive a combined score of 3–15 points, with lower scores representing a more unfavourable clinical status.

### Radiological data

For this study a single CT brain performed on the date closest to the ICP monitoring and prior to CSF diversion (if performed) was reviewed by a fellowship trained radiologist (HC) who was blinded to the patients' clinical and ICP monitoring data. The CT scans were performed on 64 slice helical scanners (LightSpeed, General Electric healthcare, Wauwatosa, WI, USA,  $n = 103$ ; or Somatom Definition AS, Siemens Healthineers, Erlangen, Germany,  $n = 14$ ). The imaging protocols utilised consisted of reformatted coronal, sagittal, and transaxial planes at a slice thickness of 5 mm, reconstructed from raw data 1 mm slices, obtained at 120 kVp and a tube current of 190–260 mA.

The Evans index was calculated from the single transaxial image (aligned to the anterior and posterior commissures) with the maximum width of the frontal horns as: (width of the frontal horns)/(biparietal diameter) [26]. The frontal occipital horn ratio (FOHR) was calculated from the transaxial slices with the maximum width for each measurement as: (width of frontal horns + width of occipital horns)/(biparietal diameter  $\times 2$ ) [27]. The callosal angle was calculated on the coronal image perpendicular to the transaxial images at the level of the posterior commissure. The CT imaging was further semiquantitatively assessed for the presence of dilated sylvian fissures, compressed high convexity CSF spaces, and cortical focal sulcal dilatation. Dilated sylvian fissures were assessed on coronal images at the central portion of the brainstem. Compressed high convexity CSF spaces were assessed on both coronal and the ten most cranial transaxial slices. Also, the cranial most slices were used to assess for cortical focal sulcal dilatation. All three parameters were graded as described in Table 1. The DESH score was then calculated according to Shinoda et al. (Table 1) [28].

This score assigns 0–2 points to the five components of DESH, leading to a composite score of 0–10 points. Higher scores represent more severe imaging findings of iNPH.

### ICP monitoring and data recording

Patients underwent diagnostic ICP monitoring as part of routine clinical management. An ICP transducer was inserted through a right frontal burr hole (Codman microsensor ICP transducer, Codman & Shurtleff, Raynham, MA, USA) [29]. ICP monitoring was performed on a neurosurgical ward for 1 night. The ICP raw data signal

**Table 1** Calculation of DESH score

Score	Definition
Ventricle size	
0	< 0.3 Evans index
1	0.3–0.35 Evans index
2	> 0.35 Evans index
Callosal angle	
0	> 100°
1	90°–100°
2	< 90°
Parasagittal CSF spaces	
0	Normal
1	Slight compression
2	Definitive compression
Sylvian fissure dilatation	
0	Normal
1	Slight dilatation or unilateral
2	Bilateral dilatation
Focal cortical sulcal dilatation	
0	Not present
1	Some present
2	Many present

DESH, disproportionately enlarged subarachnoid space hydrocephalus; CSF, cerebrospinal fluid

was digitally sampled using ICM-plus software (Cambridge University, Cambridge, UK). During the study period the raw data sampling frequency increased from 50 to 200 Hz and 1 patient was recorded at 50 Hz, 12 patients at 100 Hz and 104 patients at 200 Hz. This did not influence the frequency analysis of ICP variability, which is contained in 0.005–20 Hz. To minimise artefacts in the ICP signal only overnight data during the patients' sleep from a 10 h period from approximately 21:00–07:00 was analysed. Artefacts caused by for example temporary disconnection of the ICP probe were manually eliminated after visual inspection of the ICP raw data.

### ICP waveform parameters

We used ICM-plus software version 8.3 for the calculation of the following parameters from the 10-h overnight monitoring. For each parameter the average value from the 10-h overnight monitoring was used for analysis.

1. The mean ICP.
2. The heartbeat related ICP pulse pressure amplitude (AMP) was calculated from the amplitude of the fundamental harmonic in the frequency range of 30–140 beats per minute (bpm) over 10 s intervals and averaged every 60 s.

3. The RAP-index is a marker of cerebrospinal compensatory reserve capacity and indirectly compliance [30, 31]. It was calculated as the moving Pearson correlation coefficient between 30 consecutive samples of ICP and AMP averaged over 10 s. This 5 min time window was updated every 60 s. A low RAP indicates intact reserve capacity when the physiological slow wave fluctuations of ICP do not induce significant changes in AMP. Higher RAP suggests depleted compensatory reserve when AMP correlates with slow wave ICP oscillations.
4. The ICP amplitude of the respiration induced waves (RESP) was calculated from the amplitude of the fundamental harmonic in the frequency range of 7–30 bpm over a 120 s time window and updated every 60 s.
5. The amplitude of the slow vasogenic waves of the ICP signal (SLOW) was calculated from the square root of the power in the frequency range of 0.3–3 bpm over a 10 min time window updated every 60 s [32].

In addition, the ICP raw data was analysed in the time domain using Sensometrics software (Sensometrics 4.0.2.4, dPCom A/S, Oslo, Norway). The following parameters were calculated:

6. The heartbeat related ICP mean pulse pressure wave amplitude (MWA): The software algorithm identifies the amplitude of each single heartbeat induced pressure wave in the continuous ICP signal (the difference between diastolic minimum and systolic maximum pressure). MWA is calculated as the mean ICP pulse pressure wave amplitude for consecutive 6 s time windows. The software algorithm also identifies artefacts and time windows containing less than four valid heartbeat induced ICP waves are excluded.
7. The rise time coefficient of the ICP pulse pressure wave (RTc) was calculated as the ratio of the amplitude over the rise time of each heartbeat induced ICP wave for consecutive 6 s time windows.

### Statistical analysis

Correlation between selected parameters was calculated using non-parametric Spearman correlation coefficient with adjustment for multiple comparisons using the Benjamini–Hochberg procedure to control the false discovery rate. We calculated multiple linear regression models using a stepwise forward selection method to assess for independent explanatory variables of the dependent variable. The probability of a type-1 error ( $\alpha$ ) of 5% was accepted as being statistically significant. We used Prism software (Version 8.4.2, GraphPad LLC, San Diego, CA, USA) and Statistica software (Version 13, Tibco, Santa Clara, CA, USA) for statistical analysis.

### Results

117 patients undergoing evaluation for iNPH were included in this study. The average age was  $77.5 \pm 6.6$  years. 36 patients were female. The median combined Oslo score was 11 (interquartile range (IQR) 9.5–12, range 4–14), with the median subscore for gait 3 (IQR 2–3, range 1–5), for continence 4 (IQR 3–5, range 1–5), and for cognition 4 (IQR 3–4, range 2–5).

Table 2 shows the radiological data obtained from 117 CT scans. The average time between the CT brain used for analysis for this study and ICP monitoring was  $13 \pm 46$  days (median—1 day, range—34–270 days).

Figure 2 shows an individual example of typical 10-h overnight ICP monitoring and the waveform derived parameters AMP, RAP, RESP and SLOW. Table 3 shows the ICP waveform characteristics obtained from overnight monitoring from 117 patients. The duration of artefact free ICP data obtained during the 10-h overnight monitoring was  $594 \pm 33$  min (range 249–600 min).

### Relationship between radiological morphological and ICP waveform data

Table 4 shows the correlations between radiological morphological parameters and ICP derived parameters. The Evans Index and FOHR correlated significantly with SLOW. The DESH score showed correlations with SLOW, ICP and RESP. The degree of parasagittal CSF space compression, dilated sylvian fissures and focal sulcal dilatation all correlated with SLOW, parasagittal CSF

**Table 2** Radiological data from 117 patients included in the study

Frontal horn width (mm)	Biparietal diameter (mm)	Occipital horn width (mm)	Evans index (AU)	FOHR (AU)
51 ± 6	132 ± 6	80 ± 7	0.38 ± 0.04	0.49 ± 0.04
Callosal angle (degree)	Sylvian fissure dilatation (score)	Parasagittal CSF spaces (score)	Focal sulcal dilatation (score)	DESH score
81 ± 23	1 (0–2)	0 (0–2)	0 (0–2)	5 (0–10)

Values are mean ± standard deviation or median and range

FOHR, frontal occipital horn ratio; DESH, disproportionately enlarged subarachnoid space hydrocephalus

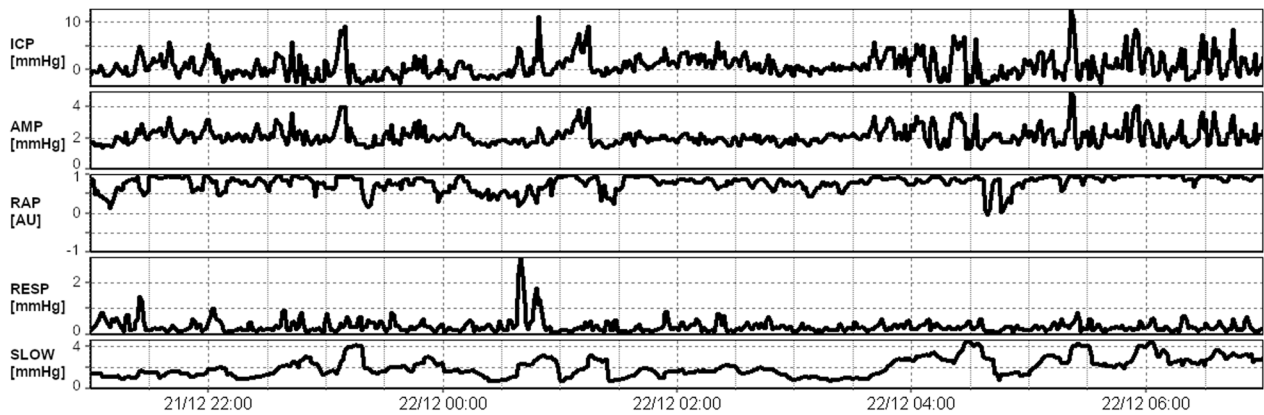


**Fig. 2** Typical 10 h overnight recording of ICP, AMP, RAP, RESP and SLOW

**Table 3** ICP monitoring data from 117 patients included in the study

ICP (mmHg)	AMP (mmHg)	MWA (mmHg)	RAP (AU)	RESP (mmHg)	SLOW (mmHg)	RTc (mmHg/s)
4.2 ± 3.8	2.3 ± 0.9	5.9 ± 2.2	0.65 ± 0.15	0.54 ± 0.26	1.60 ± 0.49	25.2 ± 10.6

Values are mean ± standard deviation

ICP, intracranial pressure; AMP, heartbeat related ICP pulse pressure amplitude calculated in the frequency domain; MWA, heartbeat related ICP pulse pressure amplitude calculated in the time domain; RAP, index of cerebrospinal reserve capacity; RESP, amplitude of the respiration related ICP waves; SLOW, amplitude of the vasogenic slow ICP waves; RTc, rise time coefficient of the heartbeat related ICP pulse pressure wave

**Table 4** Spearman correlation coefficients (r) between radiological and intracranial pressure derived variables from 117 patients

	Evans index	FOHR	Callosal angle	Parasagittal CSF spaces	Sylvian fissure dilatation	Focal cortical sulcal dilatation	DESH score
ICP (mmHg)	r = 0.03 (- 0.15 to 0.22) p = 0.81	r = 0.02 (- 0.17 to 0.20) p = 0.90	r = - 0.14 (- 0.32 to 0.05) p = 0.34	<b>r = 0.29</b> <b>(0.11–0.45)</b> <b>p = 0.016</b>	r = 0.16 (- 0.03 to 0.34) p = 0.23	r = 0.22 (0.04–0.39) p = 0.08	<b>r = 0.25</b> <b>(0.07–0.42)</b> <b>p = 0.037</b>
AMP (mmHg)	r = - 0.04 (- 0.22 to 0.15) p = 0.81	r = - 0.04 (- 0.22 to 0.15) p = 0.81	r = 0.01 (- 0.09 to 0.28) p = 0.59	r = - 0.02 (- 0.20 to 0.17) p = 0.90	r = - 0.09 (- 0.27 to 0.10) p = 0.65	r = 0.06 (- 0.13 to 0.24) p = 0.81	r = - 0.05 (- 0.23 to 0.14) p = 0.81
MWA (mmHg)	r = - 0.05 (- 0.23 to 0.14) p = 0.81	r = - 0.04 (- 0.22 to 0.15) p = 0.81	r = 0.12 (- 0.07 to 0.30) p = 0.49	r = - 0.03 (- 0.22 to 0.15) p = 0.81	r = - 0.06 (- 0.25 to 0.12) p = 0.81	r = 0.06 (- 0.13 to 0.24) p = 0.81	r = - 0.04 (- 0.22 to 0.15) p = 0.81
RAP (AU)	r = 0.20 (0.02–0.38) p = 0.11	r = 0.10 (- 0.08 to 0.28) p = 0.57	r = - 0.01 (- 0.20 to 0.18) p = 0.93	<b>r = 0.23</b> <b>(0.04–0.40)</b> <b>p = 0.045</b>	r = 0.10 (- 0.08 to 0.28) p = 0.57	r = 0.13 (- 0.06 to 0.31) p = 0.39	r = 0.16 (- 0.03 to 0.33) p = 0.25
RESP (mmHg)	r = 0.04 (- 0.15 to 0.22) p = 0.81	r = 0.03 (- 0.15 to 0.22) p = 0.81	r = - 0.10 (- 0.28 to 0.09) p = 0.57	r = 0.17 (- 0.02 to 0.34) p = 0.21	r = 0.21 (0.02–0.38) p = 0.11	<b>r = 0.28</b> <b>(0.10–0.45)</b> <b>p = 0.016</b>	<b>r = 0.25</b> <b>(0.06–0.42)</b> <b>p = 0.038</b>
SLOW (mmHg)	<b>r = 0.23</b> <b>(0.04–0.40)</b> <b>p = 0.045</b>	<b>r = 0.26</b> <b>(0.11–0.45)</b> <b>p = 0.037</b>	r = - 0.18 (- 0.35 to 0.01) p = 0.20	<b>r = 0.39</b> <b>(0.22–0.54)</b> <b>p = 0.012</b>	<b>r = 0.32</b> <b>(0.14–0.48)</b> <b>p = 0.012</b>	<b>r = 0.44</b> <b>(0.28–0.58)</b> <b>p = 0.012</b>	<b>r = 0.44</b> <b>(0.27–0.57)</b> <b>p = 0.012</b>
RTc (mmHg/s)	r = 0.03 (- 0.15 to 0.22) p = 0.81	r = 0.002 (- 0.19 to 0.19) p = 0.98	r = 0.06 (- 0.13 to 0.25) p = 0.82	r = 0.05 (- 0.14 to 0.23) p = 0.82	r = 0.02 (- 0.17 to 0.20) p = 0.90	r = 0.07 (- 0.10 to 0.27) p = 0.65	r = 0.06 (- 0.13 to 0.24) p = 0.81

Values are Spearman correlation coefficients with 95% confidence intervals and p-values with correction for multiple comparisons using the Benjamini–Hochberg procedure. Statistically significant correlations are in bold. FOHR, frontal occipital horn ratio; CSF, cerebrospinal fluid; DESH, disproportionately enlarged subarachnoid space hydrocephalus; ICP, intracranial pressure; AMP, heartbeat related ICP pulse pressure amplitude calculated in the frequency domain; MWA, heartbeat related ICP pulse pressure amplitude calculated in the time domain; RAP, index of cerebrospinal reserve capacity; RESP, amplitude of the respiration related ICP waves; SLOW, amplitude of the vasogenic slow ICP waves; RTc, rise time coefficient of the heartbeat related ICP pulse pressure wave

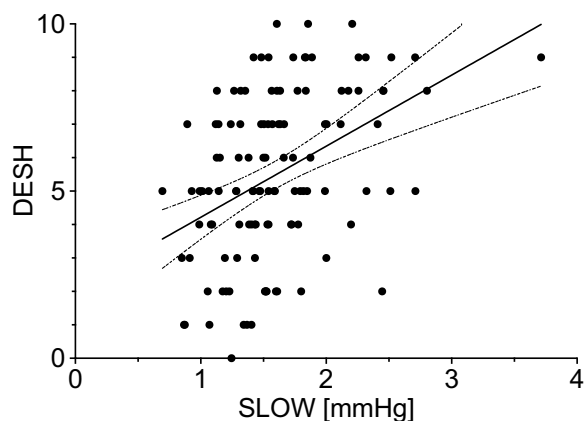


**Fig. 3** SLOW versus DESH score. Spearman  $r = 0.44$ ,  $p = 0.012$ . Linear regression line with 95% confidence intervals

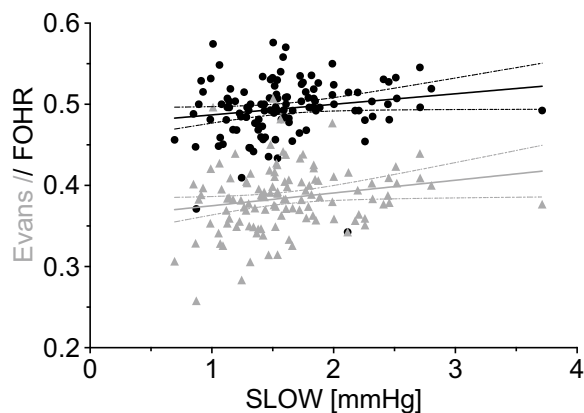


**Fig. 4** SLOW versus Evans index (grey triangles, Spearman  $r = 0.23$ ,  $p = 0.045$ ) and FOHR (black circles, Spearman  $r = 0.26$ ,  $p = 0.037$ ). Linear regression lines with 95% confidence intervals

space compression also showed correlation with ICP, RAP and RESP. There was no statistically significant correlation between AMP or MWA, measuring heartbeat related intracranial pulsations, and any of the radiological morphological variables. RTc also showed no correlations with any of the radiological morphological variables.

The strongest correlations were generally observed between SLOW and the various radiological variables, particularly with DESH. Figure 3 shows the relationship of SLOW versus DESH. Figure 4 shows the relationship of SLOW versus the variables measuring ventricle size, Evans index and FOHR.

A multiple linear regression analysis was conducted using a stepwise forward selection method with the following independent variables: age, ICP, RAP, AMP, RESP, and SLOW. The dependent variables were DESH score, Evans index, and FOHR. The models were adjusted for statistically significant interactions between independent

variables where required. As a result, three models were obtained, two of which were statistically significant. In the model with DESH as the dependent variable, after adjusting for the interaction between RAP and AMP, the model was statistically significant ( $F(1,115) = 24.5$ ,  $p < 0.0001$ , adjusted  $R^2 = 0.168$ ). Among the independent variables, only SLOW was significantly associated with DESH ( $t = 4.950$ ,  $p < 0.001$ ). Specifically, a 2.1-point increase in DESH (95% CI: 1.3–3.0) was observed for every 1 mmHg increase in SLOW. In the model with Evans index as the dependent variable, after adjusting for the interaction between SLOW and AMP, the model was statistically significant ( $F(1,115) = 4.48$ ,  $p < 0.04$ , adjusted  $R^2 = 0.03$ ), only SLOW retained predictive value ( $t = 2.12$ ,  $p < 0.04$ ). A 0.02 (CI 95%: 0.001–0.03) increase in Evans index was associated with every 1 mmHg increase in SLOW. No significant linear regression model could be built with FOHR as the dependent variable. When the variable selection method was changed from stepwise forward to one that included all effects, the model did not reach statistical significance ( $F(7,109) = 1.58$ ,  $p = 0.15$ , adjusted  $R^2 = 0.03$ ).

The Oslo score and the patients' age did not show statistically significant correlations with the radiological or the ICP derived variables.

## Discussion

This study investigated the association between radiological morphological markers of iNPH obtained from CT brain and ICP waveform characteristics obtained from overnight monitoring of ICP in 117 patients with suspected iNPH. Contrary to our initial hypothesis the amplitude of the heartbeat related ICP pulsations measured with AMP and MWA did not correlate with ventricular size. Interestingly, SLOW was the ICP waveform variable most consistently associated with the CT findings and showed the best correlation with Evans index and FOHR. Our results hence demonstrate that the magnitude of the ICP slow waves is correlated, albeit weakly, with the degree of ventricular enlargement in iNPH.

The strongest correlation in our data was between SLOW and DESH. Our results thus further demonstrate that the intensity of SLOW is significantly correlated with the severity of DESH. SLOW is a measure of the magnitude of the ICP waveform in the low frequency range of 0.3–3 bpm. The classic “b-waves” of ICP, as originally described by Lundberg at 0.5–2 bpm, are contained in this frequency range [33].

Our extended analysis window reflects the evolution of the definition of the ICP waves in the low frequency spectrum over time [34, 35]. The slow ICP waves are thought to be the effect, at least in part, of the cerebrovascular vasomotor response to slow rhythmic oscillations in

arterial blood pressure, leading to slow changes in cerebral blood volume and hence ICP [36]. Reduced intracranial compliance will amplify these slow waves, resulting in an increase of SLOW. Changes in CSF compensatory reserve, for example as induced during CSF infusion studies, also increase the amplitude of SLOW [37]. One can thus assume that SLOW is influenced by both cyclic vasogenic components, but also CSF specific components and provides some feedback about intracranial compliance.

We found statistically significant correlations between other ICP waveform components and radiological parameters. Whilst these correlations were statistically significant, the degree of correlation was often weaker. RESP demonstrated a correlation with DESH and some of its components. These respiration-induced ICP waves have not been investigated in detail, but probably provide some assessment of intracranial compliance in a faster frequency spectrum than SLOW. RAP weakly correlated with parasagittal CSF space compression. Interestingly, higher ICP itself, still in a normal range, also correlated with DESH and some of its components. We believe that all these ICP waveform variables, similar to SLOW, provide some feedback about intracranial compliance and our results suggest that impairments of intracranial compliance, as measured by the different ICP waveform components, show some association with the CT findings of iNPH.

AMP and MWA theoretically also provide a degree of compliance feedback, as they measure the pressure response to the heartbeat related increases of intracranial volume. These high frequency measures of compliance derived from the ICP waveform were not correlated with the radiological morphological findings in our data. This is possibly due to different pathophysiological mechanisms behind the pressure–volume response at volume challenges of different frequencies of the intracranial compensatory reserve system. Seminal work by Bering, Wilson and Di Rocco from the 1960 s and 1970 s indicated that the ICP pulse pressure wave caused acute ventricular enlargement in experimental hydrocephalus [21–23], however, these models are not fully adequate to mimic the processes responsible for the development of iNPH. There is also clinical data suggesting that increased arterial pulsations might be leading to large ventricles [38]. Whilst we found no association between the ICP pulse amplitude and ventricle size, we do not believe that our results necessarily contradict these earlier findings, but highlight that subacute experimental hydrocephalus and chronic iNPH of the elderly represent different pathophysiological entities. Other more recent clinical research using MRI to measure increases of heartbeat related pulsatile CSF flow in the aqueduct did also not

suggest that this is explaining the ventriculomegaly of communicating hydrocephalus [39].

Despite the numerous theories about the mechanisms of ventricular enlargement in iNPH we are not aware of pathophysiological models explaining the other components of DESH, which are steep callosal angle, parasagittal crowding, wide sylvian fissures and dilated sulci. Except for callosal angle, we found statistically significant correlations between these variables with a number of ICP waveform parameters, mainly SLOW, but also RESP, RAP, and ICP. As mentioned above, we believe that these waveform changes indicate a degree of compliance impairment and our data indicates an association between DESH and abnormal intracranial pressure–volume compensation mechanisms.

It is also a striking feature that the sylvian fissure and sulcal dilatation of iNPH seems to occur in proximity to the large arteries contained in these structures. One can hypothesise that the increase of vasogenic slow wave oscillations transmitted by these large arteries in the presence of age-related impaired compliance and increased vascular stiffness might lead to the progressive dilatation of their respective fissures and sulci with compression of the brain towards the vertex. This phenomenon seems not to be triggered by the heartbeat related arterial pulsations, but by the severity of the rhythmic vasocyclic oscillations in the slow frequency range. One could then also further revisit the role of the choroidal artery pulsations in ventricular enlargement, but focus on the slow wave frequency spectrum, again assuming that the age-related changes of intracranial compliance and vascular stiffness affecting slow wave pressure compensation possibly trigger the ventricular enlargement. It is nonetheless difficult to put these limited findings into a comprehensive pathophysiological explanation for DESH and ventricular enlargement, but it might open avenues for future research investigating the importance of ICP slow wave regulation.

The observed correlations between ICP and CT parameters do not imply causation, meaning we cannot assume based on these statistically significant correlations that an increase of ICP slow wave activity causes DESH or large ventricles. It is also possible that SLOW is increased as a result of the larger ventricles and not vice versa. We possibly also just measured two associated aspects of iNPH without a pathophysiological connection. Yet, in the regression models SLOW is associated with DESH and Evans index, which reveal an association that should not be over-interpreted but warrants further investigation. The observed statistically significant correlations between the radiological and ICP parameters were weak to moderate only; still, given the vastly different nature of the analysed morphological and physiological parameters

stronger correlations are seldom observed in this field [40].

This study has several other limitations. We used CT for the calculation of ventricle size and DESH. Magnetic resonance imaging (MRI) provides better soft tissue contrast and possibly better spatial resolution for the assessment of these iNPH specific parameters. However, data by Kockum et al. suggests that CT provides very similar results to MRI for assessing Evans index and the components of DESH [41]. Only periventricular white matter changes are typically better quantified on MRI, but did not form part of this study. It is thus unlikely that our results would have been significantly different with the use of MRI.

The ICP monitoring was done on average 13 days after the CT brain, but the median was 1 day prior to the CT brain. In 76 patients the scans used for analysis for this study were done after the ICP monitoring, often the day after ICP probe insertion. The CT was generally obtained for intraoperative navigated insertion of the ventricular catheter after the indication for VP-Shunt insertion was established. It is possible that the surgical intervention of the ICP probe insertion might have influenced the radiological morphological findings of iNPH on the analysed CT scans.

Despite its invasive nature the monitoring of ICP in iNPH generally has a low risk of adverse events [29]. A recent review and meta-analysis of diagnostic tests for iNPH in fact suggested that ICP waveform analysis is the most effective predictor for VP-shunt response [42]. Our study, however, was not intended to evaluate the complex issue of the predictive value of the analysed variables for neurological improvement after VP-Shunt insertion and to separate shunt responders from non-responders. We were aiming to investigate possible pathophysiological mechanisms, revealed by ICP waveform analysis, behind ventricular enlargement and DESH and thus did not include clinical outcome data in the analysis.

## Conclusions

Increased cerebral vasomotion, manifested by SLOW, was the main variable correlating with the morphological radiological features of iNPH on brain CT. Higher SLOW predicted a higher DESH score and larger Evans index. Heartbeat related pulsations, as measured by AMP or MWA, were not associated with ventricle size or DESH.

## Abbreviations

iNPH	Idiopathic normal pressure hydrocephalus
CSF	Cerebrospinal fluid
ICP	Intracranial pressure
CT	Computed tomography
MRI	Magnetic resonance imaging
DESH	Disproportionately enlarged subarachnoid space hydrocephalus
FOHR	Frontal occipital horn ratio

AMP	Intracranial pulse pressure amplitude calculated in the frequency domain
bpm	Beats per minute
RAP	Correlation coefficient (R) between amplitude (A) and pressure (P), a marker of cerebrospinal compensatory reserve capacity
RESP	ICP amplitude of the respiration induced waves
SLOW	Amplitude of the slow vasogenic waves of ICP
MWA	Intracranial pulse pressure mean wave amplitude calculated in the time domain
RTc	Rise time coefficient of the ICP pulse pressure wave
IQR	Interquartile range

## Acknowledgements

No acknowledgements.

## Previous presentations

Parts of this paper were presented in oral form at the Annual Scientific Meeting of the Neurosurgical Society of Australasia in Sydney, Australia, September 2022, the 18th International Symposium on Intracranial Pressure and Brain Monitoring in Cape Town, South Africa, November 2022, and the 15th Meeting of the Hydrocephalus Society in Hamburg, Germany, August 2023.

## Author contributions

RTM planned the study, collected, analysed and interpreted data and critically revised the manuscript. HC collected data and critically revised the manuscript. MK critically reviewed the data, performed the statistical analysis and revised the manuscript. CRV collected data and critically revised the manuscript. MC critically reviewed the data and revised the manuscript. ZC critically reviewed the data and revised the manuscript. MJ conceptualised and planned the study, collected, analysed and interpreted data and drafted the manuscript. All authors read and approved the final manuscript.

## Funding

This study did not receive specific funding.

## Data availability

The data that support the findings of this study are available upon reasonable request from the corresponding author [MJ]. The data are not publicly available due to them containing information that could compromise research participant privacy.

## Declarations

### Ethics approval and consent to participate

The joint human research ethics committee of the University of Wollongong and the Illawarra Shoalhaven Local Health District approved this study (ISLHD/LNR/2020-083). Because of the retrospective nature of the study with analysis of routinely collected data and long study time the need for informed consent was waived.

### Consent for publication

Not applicable.

### Competing interests

MC has partial financial interest from ICM + software purchase licenses.

### Author details

<sup>1</sup>Department of Neurosurgery, Wollongong Hospital, Loftus Street, Wollongong, NSW 2500, Australia. <sup>2</sup>Graduate School of Medicine, University of Wollongong, Wollongong, NSW, Australia. <sup>3</sup>Department of Medical Imaging, Wollongong Hospital, Wollongong, NSW, Australia. <sup>4</sup>Department of Biomedical Engineering, Faculty of Fundamental Problems of Technology, Wrocław University of Science and Technology, Wrocław, Poland. <sup>5</sup>Department of Clinical Neurosciences, Addenbrooke's Hospital and University of Cambridge, Cambridge, UK. <sup>6</sup>Institute of Electronic Systems, Warsaw University of Technology, Warsaw, Poland.

Received: 30 November 2024 Accepted: 1 June 2025

Published online: 18 June 2025

## References

- Andrén K, Wikkelsø C, Tisell M, Hellström P. Natural course of idiopathic normal pressure hydrocephalus. *J Neurol Neurosurg Psychiatry*. 2014;85(7):806–10.
- Jaraj D, Wikkelsø C, Rabiei K, et al. Mortality and risk of dementia in normal-pressure hydrocephalus: A population study. *Alzheimers Dement*. 2017;13(8):850–7.
- Klinge P, Hellström P, Tans J, Wikkelsø C. One-year outcome in the European multicentre study on iNPH. *Acta Neurol Scand*. 2012;126(3):145–53.
- Kazui H, Miyajima M, Mori E, Ishikawa M. Lumboperitoneal shunt surgery for idiopathic normal pressure hydrocephalus (SINPHONI-2): an open-label randomised trial. *Lancet Neurol*. 2015;14(6):585–94.
- Chidiac C, Sundström N, Tullberg M, Arvidsson L, Olivecrona M. Waiting time for surgery influences the outcome in idiopathic normal pressure hydrocephalus—a population based study. *Acta Neurochir (Wien)*. 2022;164(2):469–78.
- Borgesen SE, Gjers F. The predictive value of conductance to outflow of CSF in normal pressure hydrocephalus. *Brain*. 1982;105:65–86.
- Greitz D. Radiological assessment of hydrocephalus: new theories and implications for therapy. *Neurosurg Rev*. 2004;27(3):145–65.
- Jaraj D, Rabiei K, Marlow T, Jensen C, Skoog I, Wikkelsø C. Prevalence of idiopathic normal-pressure hydrocephalus. *Neurology*. 2014;82(9):1449–54.
- Bannister CM. A report of eight patients with low pressure hydrocephalus treated by CSF diversion with disappointing results. *Acta Neurochir (Wien)*. 1972;27(1):1–5.
- Vanneste J, Augustijn P, Dirven C, Tan WF, Goedhart ZD. Shunting normal-pressure hydrocephalus: do the benefits outweigh the risks? A multicenter study and literature review. *Neurology*. 1992;42(1):54–9.
- Espay AJ, Da Prat GA, Dwivedi AK, et al. Deconstructing normal pressure hydrocephalus: Ventriculomegaly as early sign of neurodegeneration. *Ann Neurol*. 2017;82(4):503–13.
- Hashimoto M, Ishikawa M, Mori E, Kuwana N. Diagnosis of idiopathic normal pressure hydrocephalus is supported by MRI-based scheme: a prospective cohort study. *Cerebrospinal Fluid Res*. 2010;7:18.
- Symon L, Dorsch NW, Stephens RJ. Pressure waves in so-called low-pressure hydrocephalus. *Lancet*. 1972;2(7790):1291–2.
- Nornes H, Rootwelt K, Sjaastad O. Normal pressure hydrocephalus. Long-term intracranial pressure recording. *Eur Neurol*. 1973;9(5):261–174.
- Chawla JC, Hulme A, Cooper R. Intracranial pressure in patients with dementia and communicating hydrocephalus. *J Neurosurg*. 1974;40(3):376–80.
- Qvarlander S, Lundkvist B, Koskinen LOD, Malm J, Eklund A. Pulsatility in CSF dynamics: pathophysiology of idiopathic normal pressure hydrocephalus. *J Neurol Neurosurg Psychiatry*. 2013;84(7):735–41.
- Eide PK, Sorteberg W. Diagnostic intracranial pressure monitoring and surgical management in idiopathic normal pressure hydrocephalus: a 6-year review of 214 patients. *Neurosurgery*. 2010;66(1):80–91.
- Green LM, Wallis T, Schuhmann MU, Jaeger M. Intracranial pressure waveform characteristics in idiopathic normal pressure hydrocephalus and late-onset idiopathic aqueductal stenosis. *Fluids Barriers CNS*. 2021;18(1):25.
- Raftopoulos C, Chaskis C, Delecluse F, Cantraine F, Bidaut L, Brothi J. Morphological quantitative analysis of intracranial pressure waves in normal pressure hydrocephalus. *Neurol Res*. 1992;14(5):389–96.
- Graff-Radford NR, Godersky JC, Jones MP. Variables predicting surgical outcome in symptomatic hydrocephalus in the elderly. *Neurology*. 1989;39(12):1601–4.
- Bering EA. Circulation of the cerebrospinal fluid. Demonstration of the choroid plexuses as the generator of the force for flow of fluid and ventricular enlargement. *J Neurosurg*. 1962;19(5):405–13.
- Wilson CB, Bertan V. Interruption of the anterior choroidal artery in experimental hydrocephalus. *Arch Neurol*. 1967;17(6):614–9.
- Di Rocco C, Pettorossi VE, Caldarelli M, Mancinelli R, Velardi F. Communicating hydrocephalus induced by mechanically increased amplitude of the intraventricular cerebrospinal fluid pressure: Experimental studies. *Exp Neurol*. 1978;59(1):40–52.
- Relkin N, Marmarou A, Klinge P, Bergsneider M, Black PM. Diagnosing idiopathic normal-pressure hydrocephalus. *Neurosurgery*. 2005;57(3 Suppl):S4–16.
- Eide PK. Intracranial pressure parameters in idiopathic normal pressure hydrocephalus patients treated with ventriculo-peritoneal shunts. *Acta Neurochir (Wien)*. 2006;148(1):21–19.
- Evans WA. An encephalographic ratio for estimating ventricular enlargement and cerebral atrophy. *Arch Neurol Psychiatry*. 1942;47(6):931–7.
- O'Hayon BB, Drake JM, Ossip MG, Tuli S, Clarke M. Frontal and occipital horn ratio: A linear estimate of ventricular size for multiple imaging modalities in pediatric hydrocephalus. *Pediatr Neurosurg*. 1998;29(5):245–9.
- Shinoda N, Hirai O, Hori S, et al. Utility of MRI-based disproportionately enlarged subarachnoid space hydrocephalus scoring for predicting prognosis after surgery for idiopathic normal pressure hydrocephalus: clinical research. *J Neurosurg*. 2017;127(6):1436–42.
- Vonhoff CR, Wallis T, Jaeger M. Complications of elective intracranial pressure monitoring in adult hydrocephalus. *J Clin Neurosci*. 2020;79:67–70.
- Czosnyka M, Guazzo E, Whitehouse M, et al. Significance of intracranial pressure waveform analysis after head injury. *Acta Neurochir (Wien)*. 1996;138(5):531–41.
- Kim D-J, Czosnyka Z, Keong N, et al. Index of cerebrospinal compensatory reserve in hydrocephalus. *Neurosurgery*. 2009;64(3):494–502.
- Balestreri M, Czosnyka M, Steiner LA, et al. Intracranial hypertension: what additional information can be derived from ICP waveform after head injury? *Acta Neurochir (Wien)*. 2004;146(2):131–41.
- Lundberg N. Continuous recording and control of ventricular fluid pressure in neurosurgical practice. *Acta Psychiatr Scand Suppl*. 1960;36(149):1–193.
- Spiegelberg A, Preuß M, Kurtcuoglu V. B-waves revisited. *Interdiscip Neurosurg: Adv Tech Case Manag*. 2016;6:13–7.
- Martinez-Tejada I, Arum A, Wilhelm JE, Juhler M, Andresen M. B waves: a systematic review of terminology, characteristics, and analysis methods. *Fluids Barriers CNS*. 2019;16(1):33.
- Newell DW, Aaslid R, Stooss R, Reulen HJ. The relationship of blood flow velocity fluctuations to intracranial pressure B waves. *J Neurosurg*. 1992;76(3):415–21.
- Momjian S, Czosnyka Z, Czosnyka M, Pickard JD. Link between vasogenic waves of intracranial pressure and cerebrospinal fluid outflow resistance in normal pressure hydrocephalus. *Br J Neurosurg*. 2004;18(1):56–61.
- Graff-Radford NR, Knopman DS, Penman AD, Coker LH, Mosley TH. Do systolic BP and pulse pressure relate to ventricular enlargement? *Eur J Neurol*. 2013;20(4):720–4.
- Holmlund P, Qvarlander S, Malm J, Eklund A. Can pulsatile CSF flow across the cerebral aqueduct cause ventriculomegaly? A prospective study of patients with communicating hydrocephalus. *Fluids Barriers CNS*. 2019;16(1):40.
- Czosnyka Z, Czosnyka M, Pickard JD. CSF Pulse Pressure and B Waves. *J Neurosurg*. 2005;103(4):767.
- Kockum K, Virhammar J, Riklund K, Söderström L, Larsson EM, Laurell K. Standardized image evaluation in patients with idiopathic normal pressure hydrocephalus: consistency and reproducibility. *Neuroradiology*. 2019;61(12):1397–406.
- Thavarajasingam SG, El-Khatib M, Rea M, et al. Clinical predictors of shunt response in the diagnosis and treatment of idiopathic normal pressure hydrocephalus: a systematic review and meta-analysis. *Acta Neurochir (Wien)*. 2021;163(10):2641–72.

## Publisher's Note

Springer Nature remains neutral with regard to jurisdictional claims in published maps and institutional affiliations.